# Fresnel Filtering in Lasing Emission from Scarred Modes of Wave-Chaotic Optical Resonators

N. B. Rex, H. E. Tureci, H. G. L. Schwefel, R. K. Chang, and A. Douglas Stone

*Department of Applied Physics, P.O. Box 208284, Yale University, New Haven, Connecticut 06520-8284*

We study lasing emission from asymmetric resonant cavity GaN microlasers. By comparing far-field intensity patterns with images of the microlaser we find that the lasing modes are concentrated on three-bounce unstable periodic ray orbits; i.e., the modes are scarred. The high-intensity emission directions of these scarred modes are completely different from those predicted by applying Snell's law to the ray orbit. This effect is due to the process of "Fresnel filtering" which occurs when a beam of finite angular spread is incident at the critical angle for total internal reflection.

Understanding the correspondence between classical phase-space structures and wave functions for a general classical dynamics is the goal of investigations in quantum/wave chaotic systems [1]. Generic Hamiltonian systems have mixed phase spaces which consist of tori (which support quasiperiodic orbits), stable periodic orbits with their associated islands of stability, and unstable periodic orbits which lie in regions of phase space with chaotic motion. The simplest possibility, explored in the early days of the field, was that quantum wave functions, when projected into phase space, would cover approximately uniformly each type of region of phase space. We now know [2] that this situation is realized only at extremely high quantum numbers and that there exist states ("scars") in the chaotic region which remain localized on unstable classical periodic orbits instead of filling the chaotic component uniformly [3,4]. The same considerations which lead to scarred eigenstates of the Schrödinger equation also imply that the wave equation of electromagnetism will have scarred modes when its boundary conditions (e.g., shape of a resonator) generate chaotic ray motion; and indeed such modes have been previously observed in microwave cavities [5].

It has been shown that dielectric *optical* microcavities and microlasers represent a realization of a wave-chaotic system and one that presents many unsolved problems for optical physics [6–9]. For example, quadrupole-deformed InGaAs and GaAs quantum cascade microlasers which lased on stable bow-tie modes were found to produce 1000 times higher output power than undeformed cylindrical lasers of the same type [8,9]. The mechanism of mode selection and the increase of output power in these devices is not currently understood. Recently we reported preliminary data [10,11] indicating that in deformed GaN diode lasers the stable bow-tie modes are not selected but instead unstable "triangle" modes are dominant. This was the first time that scars had been observed in an active as opposed to a passive cavity.

In this Letter we present newer and more complete data which show that the emission pattern of these triangular scarred modes is completely different from that expected by applying Snell's law to the underlying periodic orbit. Below we interpret this surprising finding as due to an effect we term "Fresnel filtering" (FF) which arises when a beam of finite angular spread is partially transmitted through a dielectric interface near the total internal reflection condition. This is a generic violation of ray optics for a focused beam, somewhat similar to the well-studied Goos-Hänchen shift for a reflected beam [12,13], which has not to our knowledge been identified in the optics literature. We are able to clearly identify this effect since we simultaneously collect far-field emission patterns *and* images of the sidewall of the resonator. Two other groups have very recently reported lasing emission from dielectric microcavities which they interpret as due to scarred modes [14,15]; these groups do not study the FF effect we focus on here.

The experimental setup is shown schematically in Fig. 1(a). A GaN microlaser of refractive index $n = 2.65$ is optically pumped at 355 nm and emits at 375 nm. The structure is based on GaN grown by metal-organic chemical vapor deposition (MOCVD) on a sapphire substrate which is etched from a mask using standard photolithography to create a 2 $\mu$m high pillar with a quadrupolar deformation of the cross section, $r(\phi) = r_0(1 + \epsilon \cos 2\phi)$ with $r_0 = 100$ $\mu$m. Light emitted from the laser is imaged through an aperture subtending a 5° angle and lens onto a charge-coupled device (CCD) camera which is rotated by an angle $\theta$ in the far field from the major axis. A bandpass filter restricts the imaged light to the stimulated emission region of the GaN spectrum. The CCD camera records an image of the intensity profile on the sidewall of the pillar as viewed from the angle $\theta$ which is converted from pixels to angular position $\phi_W$. Summing these intensities yields the total far-field intensity emitted in direction $\theta$. Data were taken for quadrupole lasers with $\epsilon = 0.12, 0.14, 0.16, 0.18$, and 0.20 and for other shapes as well. The full data set will be analyzed in a later work, but here we focus on the data for $\epsilon = 0.12$ which show a simple scarred mode. In Fig. 1(b) these data are displayed in a color scale which identifies both the highest emission directions and the brightest points on the sidewall (labeled by their angle $\phi_W$).
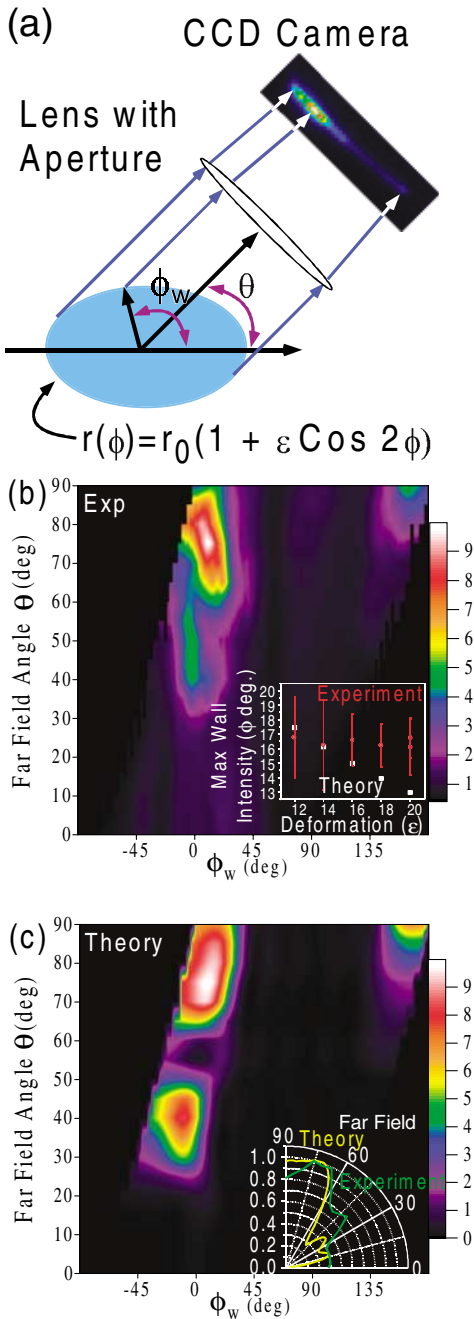
FIG. 1 (color).    (a) Experimental setup, viewed from above, for measuring simultaneously far-field intensity patterns and images of the sidewall emission. The lasing modes emit in the plane shown. (b) Experimental data showing in color scale the CCD images (converted to sidewall angle $\phi_W$) as a function of camera angle $\theta$. Three bright spots are observed on the boundary for camera angles in the 1st quadrant, at $\phi_W \approx 17°, 162°, -5°$. Inset shows the position of the bright spot in the 1st quadrant vs deformation, compared to the location of the triangular periodic orbit [see insets of Figs. 2(a) and Fig. 3(a)]. (c) Calculation of expected image data using the scarred mode shown in Fig. 2(a); inset shows calculated and experimental far-field patterns obtained by integrating over $\phi_W$ for each $\theta$.

The data show that the maximum intensity in the 1st quadrant is observed at angle $\theta \approx 74°$ and is emitted from the region of the sidewall around $\phi_W \approx 17°$; secondary

spots are observed at $\phi_W \approx -5°, 162°$. The observation of a small number of well-localized bright spots on the sidewall suggests a lasing mode based on a short periodic ray trajectory. The two-bounce stable Fabry-Perot mode would emit from $\phi_W = 90°$ in the direction $\theta = 90°$. The stable four-bounce bow-tie mode, dominant in the devices of Ref. [8], is also ruled out by our data. It is very low-$Q$ at this deformation due to its small angle of incidence and would give bright spots at $\phi_W \approx 73°, 107°$. There is, however, a pair of symmetry-related isosceles triangular orbits [inset, Fig. 2(a)] with bounce points very close to the observed bright spots [see inset of Fig. 1(b)]. These orbits are unstable for $\epsilon > 0.098$, with trace of the monodromy matrix equal to $-5.27$ at $\epsilon = 0.12$. The two equivalent bounce points in each triangle at $\phi_W = \pm 17°$ and $180° \pm 17°$ have $\sin\chi \approx 0.42$, very near to the critical value, $\sin\chi_c = 1/n = 0.38$, whereas the bounce points at $\phi_W = \pm 90°$ have $\sin\chi = 0.64$ and should emit negligibly [inset of Fig. 2(a)]. This accounts for the three bright spots observed experimentally (in the first quadrant) in Fig. 1(b). Solutions for the quasibound states of this resonator in the passive cavity can be found numerically [16], both in real space and phase space, and we find that indeed there exist such scars [see Figs. 2(a) and 2(b)]. Here we plot both the modulus of the electric field in real space and the projection of the Husimi distribution of the mode onto the surface of section of the resonator [17]. The Husimi distribution is a (Gaussian) smoothed version of the Wigner transform of the mode, which represents a wave function or mode as a phase-space density consistent with the uncertainty principle. Projection onto the surface of section then gives a measure of the density of rays which strike the boundary at a given position, $\phi_W$, and a given incidence angle, $\chi$. Additionally we evaluate this mode in the far field and find an emission pattern in good agreement with the experimental measurement [see inset, Fig. 1(c)]. Finally, if we propagate the scarred mode numerically via a lens transform [18] we obtain the result shown in Fig. 1(c), which is in quite reasonable agreement with the experimental data of Fig. 1(b), taking into account that the lasing mode should differ somewhat from the resonance of the empty cavity [16]. Hence we conclude that the dominant lasing mode in the experiment is such a scarred mode. The data of Figs. 1(a) and 1(b), however, present an intriguing puzzle from the point of view of ray optics. A mode localized on these triangular orbits would be expected to emit from the four bounce points approximately in the tangent direction according to Snell's law; this means that the bright spot at $\phi_W = 17°$ "should" emit into the direction $\theta \approx 115°$, whereas the data clearly indicate that the $17°$ bright spot emits in the direction $\theta = 72°$.

Thus the emission pattern violates the intuitive expectations of ray optics by $43°$, a huge discrepancy [see Fig. 3(a)]. Moreover, the ratio $\lambda/nR = 2.8 \times 10^{-3}$, seemingly well into the ray optics limit. The resolution of this apparent paradox is suggested by the numerical data of Fig. 2(b). It is clear that the scarred mode, while
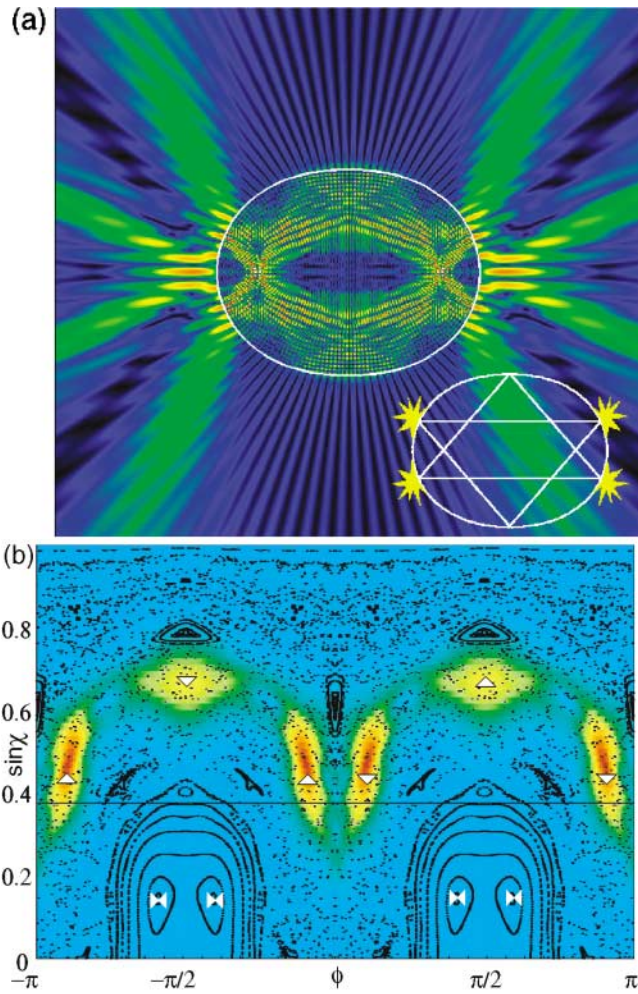
FIG. 2 (color). (a) Real-space false color plot of the modulus of the electric field for a calculated quasibound state of $nkr_o \approx 129$ ($n$ is the index of refraction, $k$ is the real part of the resonant wave vector) and $\epsilon = 0.12$ which is scarred by the triangular periodic orbits shown in the inset. The four points of low incidence angle which should emit strongly are indicated. (b) Husimi (phase-space distribution) for the same mode projected onto the surface of section (SOS) of the resonator. The $x$ axis is $\phi_W$ and the $y$ axis is $\sin\chi$, the angle of incidence at the boundary. The SOS for the corresponding ray dynamics is shown in black, indicating that there are no stable islands (orbits) near the high intensity points for this mode. Instead, the high-intensity points coincide well with the bounce points of the unstable triangular orbits (triangles). The black line denotes $\sin\chi_c = 1/n$ for GaN; the triangle orbits are just above this line and would be strongly confined, whereas the stable bow-tie orbits (bow-tie symbols) are well below and would not be favored under uniform pumping conditions.

localized around the triangle orbit, has a significant spread in the angle of incidence, $\Delta \sin\chi \approx 0.2$. This means that we can regard the scarred mode as a (non-Gaussian) beam with a large angular spread incident near the critical angle for total internal reflection. We have shown that such a beam incident on a flat interface is strongly deflected in the far field away from the tangent direction expected from Snell's law [19]; we call this effect Fresnel filtering. Since $\lambda/nR \ll 1$ here, one can neglect the curvature

corrections, and use the flat interface result to get an estimate for the expected angular shift. The far-field intensity pattern $I(\theta)$ found by the saddle-point method in [19], is of the form

$$I(\theta) \propto \left| \mathcal{T}\left( \frac{\sin\chi_e(\theta)}{n} \right) \mathcal{P}\left( \frac{\sin\chi_e(\theta)}{n} \right) J\left( \frac{\sin\chi_e(\theta)}{n} \right) \right|^2 .$$

(1)

Here $\mathcal{P}(\sin\chi)$ is the angular distribution of the incoming beam at $\chi$, $\mathcal{T}(\sin\chi) = \cos\chi/(\cos\chi + \sqrt{1 - n^2 \sin\chi^2})$ is the corresponding Fresnel transmission coefficient, and $J(\sin\chi) = \cos(\chi - \chi_i^o)\sqrt{1/n^2 - \sin\chi^2}/\cos\chi$ is the amplitude factor from the saddle-point integration. $\chi_i^o$ is the central angle of the incident "beam" and the observation direction $\theta = \chi_e(\theta)$ for the plane interface, while
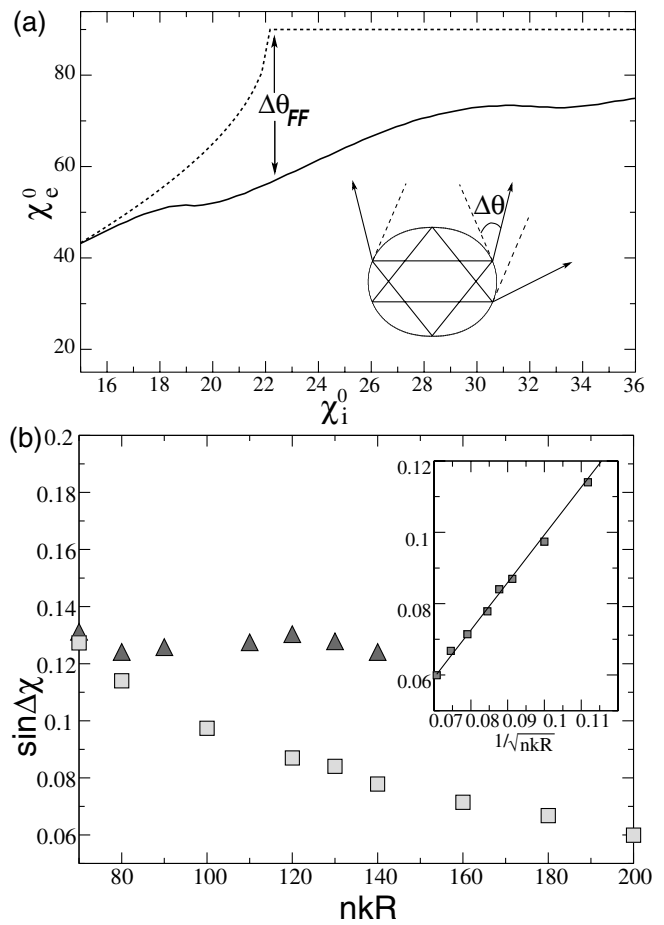


FIG. 3. (a) Solid line: Central beam emission angle $\chi_e^o$ vs central incidence angle $\chi_i^o$ for a beam of angular spread equivalent to the scarred mode of Fig. 2 incident on a plane interface. Dashed line is Snell's law, and the discrepancy is the Fresnel filtering angle $\Delta\theta_{FF}$. Inset schematic shows the three emitted "beams" detected in the experiment and illustrates their strong deviation from Snell's law (dashed tangent lines). (b) Dependence of angular spread of the "incident beams" vs $nkr_o$ for scarred triangle modes (triangles) and stable (Gaussian) bow-tie modes; inset shows that the spread decreases as $1/\sqrt{nkr_o}$ (see inset) for stable Gaussian modes as predicted, whereas no clear variation with $nkr_o$ is seen for the scarred modes.

for the equivalent resonator $\chi_e = \theta - \cos^{-1}[\hat{n}(\phi_b) \cdot \hat{x}]$, where $\hat{n}(\phi_b)$ is the unit normal at the bounce point. It is the factor $J[\sin\chi_e(\theta)/n]$ which shifts the outgoing maximum away from the Snell direction related to $\chi_i^o$. Near $\sin\chi_i^o = 1/n$, this factor is inversely proportional to the outgoing beam spread associated with a small change in the incident beam spread. It follows from Snell's law that this change becomes very large near the critical angle, causing the amplitude at tangent emission to tend to zero [19].

To model the experiment we assume that the probability distribution for the incidence angle is approximately the same as the cross section of the Husimi distribution of Fig. 2(b) evaluated at the triangle bounce point $\phi_W = 17°$. In Fig. 3 we plot the beam emission angle $\chi_e^o(\theta)$ defined as the angular maximum of the far-field pattern vs central incidence angle $\chi_i^o$. We find a very large angular shift $\Delta\theta_{FF}$, in reasonable agreement with experiment considering we have neglected curvature effects. The size of the Fresnel filtering effect depends strongly on the angular beam spread. For Gaussian resonator modes one can show that this spread tends to zero as $1/\sqrt{nkr_o}$ [19] [see inset Fig. 3(b)]. Since our numerical simulations of the scarred mode are for $nkr_o \approx 129$, whereas the experiment corresponds to $nkr_o \approx 4,440$, one may ask whether the large Fresnel filtering angle found in Fig. 3(a) (for $nkr_o \approx 129$) will extrapolate correctly to agree with the experiment. As there is currently no theory of this scaling for scarred modes, we studied the scaling of the angular width numerically [Fig. 3(b)].

We found no detectable decrease in the angular width with $nkr_o$, in clear contrast to the behavior of the Gaussian modes. It is also likely that at this high $nkr_o$ we have multimode lasing which effectively increases the angular beam width.

In conclusion, we have found that the dominant lasing mode in quadrupolar GaN microlasers are unstable (scarred) modes. For resonators with chaotic ray dynamics, such scarred modes play a special role as they allow high-$Q$ resonances despite the ray chaos. Such modes exhibit a novel emission pattern, which is completely different from that expected by applying Snell's law to the underlying periodic ray trajectory, due to the phenomenon of Fresnel filtering.

[1] M. C. Gutzwiller, *Chaos and Quantum Physics* (Springer-Verlag, New York, 1990).

[2] T. Prosen and M. Robnik, J. Phys. A **27**, 8059 (1994).

[3] E. J. Heller, Phys. Rev. Lett. **53**, 1515 (1984).

[4] L. Kaplan and E. J. Heller, Ann. Phys. (N.Y.) **264**, 171 (1998).

[5] S. Sridhar and E. J. Heller, Phys. Rev. A **46**, R1728 (1992).

[6] A. Mekis, J. U. Nöckel, G. Chen, A. D. Stone, and R. K. Chang, Phys. Rev. Lett. **75**, 2682 (1995).

[7] J. U. Nöckel and A. D. Stone, Nature (London) **385**, 45 (1997).

[8] C. Gmachl, F. Capasso, E. E. Narimanov, J. U. Nöckel, A. D. Stone, J. Faist, D. L. Sivco, and A. Y. Cho, Science **280**, 1556 (1998).

[9] S. Gianordoli, L. Hvozdara, G. Strasser, W. Schrenk, J. Faist, and E. Gornik, IEEE J. Quantum Electron. **36**, 458 (2000).

[10] N. B. Rex, R. K. Chang, and L. J. Guido, QELS 2001 Technical Digest (2001), p. 63; Proc. SPIE Int. Soc. Opt. Eng. **3930**, 163 (2000).

[11] A. D. Stone, Phys. Scr. **T90**, 248 (2001).

[12] F. Goos and H. Hänchen, Ann. Phys. (Leipzig) **1**, 333 (1947).

[13] B. R. Horowitz and T. Tamir, J. Opt. Soc. Am. **61**, 586 (1971).

[14] E. Narimanov, C. Gmachl, F. Capasso, J. N. Baillargeon, and A. Y. Cho, CLEO 2001 Technical Digest (2001), p. 195.

[15] S.-B. Lee *et al.*, physics/0106031.

[16] It is conventional for high-$Q$ laser cavities to approximate the lasing mode by the resonant mode in the absence of pumping and gain; see, e.g., A. E. Siegman, *Lasers* (University Science Books, California, 1986).

[17] S. D. Frischat and E. Doron, J. Phys. A **30**, 3613 (1997).

[18] J. W. Goodman, *Introduction to Fourier Optics* (McGraw-Hill, New York, 1996), 2nd ed.

[19] H. E. Tureci and A. D. Stone, Opt. Lett. **27**, 7 (2002).